Supplement of Atmos. Chem. Phys., 18, 2381–2394, 2018
https://doi.org/10.5194/acp-18-2381-2018-supplement


Atmospheric Chemistry and Physics
Open Access
EGU

*Supplement of*

# Temperature-(208–318 K) and pressure-(18–696 Torr) dependent rate coefficients for the reaction between OH and $HNO_3$

**Katrin Dulitz et al.**

*Correspondence to:* John Crowley (john.crowley@mpic.de)

**Supplementary Information**

**Table S1**: Experimental rate coefficients, $k_5$

| $T$ (K) | $p$ (Torr) | $k_5$ | $HNO_3$ | $T$ (K) | $p$ (Torr) | $k_5$ | $HNO_3$ | $T$ (K) | $p$ (Torr) | $k_5$ | $HNO_3$ |
|---|---|---|---|---|---|---|---|---|---|---|---|
| 208 | 20.0 | 6.30 ± 0.29 | a | 242 | 496.0 | 3.66 ± 0.07 | a | 275 | 50.0 | 1.68 ± 0.02* | w |
| 217 | 20.0 | 4.61 ± 0.06 | a | 242 | 529.7 | 3.66 ± 0.05 | w | 275 | 50.0 | 1.61 ± 0.02 | w |
| 217 | 20.0 | 4.81 ± 0.05 | a | 242 | 530.5 | 3.55 ± 0.06 | a | 277 | 99.3 | 1.75 ± 0.02 | t |
| 218 | 50.0 | 5.58 ± 0.05 | a | 245 | 294.1 | 3.12 ± 0.06 | w | 276 | 98.6 | 1.76 ± 0.02 | a |
| 217 | 50.0 | 6.13 ± 0.12 | a | 245 | 294.9 | 3.09 ± 0.07 | w | 276 | 99.4 | 1.77 ± 0.02 | w |
| 217 | 91.1 | 6.46 ± 0.10 | a | 245 | 295.1 | 3.23 ± 0.05 | w | 277 | 121.2 | 1.74 ± 0.02 | t |
| 227 | 20.0 | 4.08 ± 0.04 | a | 245 | 295.8 | 3.09 ± 0.05 | w | 278 | 196.3 | 1.71 ± 0.02 | t |
| 227 | 20.9 | 3.96 ± 0.03 | a | 245 | 296.4 | 3.23 ± 0.05 | a | 278 | 196.4 | 1.75 ± 0.03 | t |
| 227 | 50.2 | 4.72 ± 0.05 | a | 246 | 493.5 | 3.23 ± 0.07 | w | 278 | 285.0 | 1.77 ± 0.01 | w |
| 227 | 146.1 | 5.13 ± 0.10 | a | 257 | 20.0 | 2.00 ± 0.02 | a | 278 | 296.0 | 1.77 ± 0.03 | t |
| 227 | 296.1 | 5.46 ± 0.21 | a | 257 | 23.7 | 2.14 ± 0.02 | w | 278 | 296.8 | 1.78 ± 0.02 | a |
| 227 | 495.9 | 5.84 ± 0.18 | a | 257 | 50.0 | 2.23 ± 0.02 | a | 277 | 398.2 | 1.75 ± 0.02 | t |
| 239 | 17.7 | 3.09 ± 0.03 | w | 257 | 99.9 | 2.41 ± 0.02 | w | 276 | 500.9 | 1.82 ± 0.02 | w |
| 239 | 17.9 | 3.01 ± 0.03 | w | 257 | 300.1 | 2.55 ± 0.03 | a | 275 | 601.8 | 1.84 ± 0.02 | w |
| 239 | 18.2 | 3.07 ± 0.05 | w | 257 | 300.6 | 2.54 ± 0.03 | w | 297 | 18.1 | 1.26 ± 0.02 | a |
| 239 | 19.5 | 3.09 ± 0.07 | w | 257 | 400.8 | 2.54 ± 0.03 | w | 297 | 20.0 | 1.23 ± 0.01* | w |
| 239 | 49.4 | 3.54 ± 0.03 | w | 257 | 499.3 | 2.48 ± 0.04 | a | 297 | 27.3 | 1.24 ± 0.01 | w |
| 239 | 49.8 | 3.54 ± 0.06 | w | 257 | 562.5 | 2.56 ± 0.03 | w | 297 | 50.0 | 1.29 ± 0.01 | w |
| 239 | 49.8 | 3.53 ± 0.03 | w | 276 | 17.9 | 1.59 ± 0.02 | a | 297 | 98.7 | 1.35 ± 0.02 | a |
| 239 | 50.1 | 3.53 ± 0.04 | a | 276 | 18.2 | 1.69 ± 0.03 | t | 298 | 220.5 | 1.38 ± 0.01 | t |
| 239 | 50.2 | 3.61 ± 0.04 | w | 276 | 18.2 | 1.67 ± 0.02 | t | 297 | 296.3 | 1.40 ± 0.02 | t |
| 239 | 49.7 | 3.40 ± 0.04 | w | 276 | 18.3 | 1.60 ± 0.02 | w | 297 | 301.2 | 1.36 ± 0.01 | w |
| 242 | 20.0 | 2.74 ± 0.04 | a | 275 | 20.0 | 1.56 ± 0.02* | w | 298 | 396.6 | 1.40 ± 0.01 | t |
| 242 | 22.3 | 2.81 ± 0.02 | w | 275 | 20.0 | 1.60 ± 0.02 | w | 297 | 500.6 | 1.38 ± 0.01 | w |
| 242 | 50.2 | 3.19 ± 0.05 | a | 276 | 25.3 | 1.62 ± 0.01 | w | 297 | 650.2 | 1.39 ± 0.02 | w |
| 242 | 99.0 | 3.40 ± 0.05 | w | 276 | 35.1 | 1.67 ± 0.01 | t | 318 | 29.2 | 1.05 ± 0.01 | w |
| 242 | 99.2 | 3.47 ± 0.04 | w | 275 | 35.4 | 1.71 ± 0.02 | t | 319 | 696.1 | 1.12 ± 0.01 | w |
| 242 | 146.1 | 3.54 ± 0.05 | a | 275 | 36.2 | 1.71 ± 0.02 | t | | | | |
| 242 | 296.3 | 3.63 ± 0.07 | a | 275 | 40.1 | 1.68 ± 0.01 | a | | | | |
| | | | | | | | | | | | |
| | | | | | | | | | | | |
| | | | | | | | | | | | |

Units of $k_5$ are $10^{-13}$ $cm^3$ $molecule^{-1}$ $s^{-1}$, measurements in synthetic air are marked with an asterisk, errors are statistical only (two standard deviations); abbreviations: a = anhydrous $HNO_3$, w = 90 % $HNO_3$, t = ternary mixture

**TPEFS detection of $HNO_3$: Correction of data due to fluorescence quenching and absorption of excitation light by $HNO_3$.**

In this section, we describe in detail the method used to correct the TPEFS signal as a function of [$HNO_3$]. At high $HNO_3$ concentrations (>$10^{14}$ $cm^{-3}$) relevant for this study, 193 nm light absorption between the entrance Brewster window and the excitation volume at the centre of the reactor can reduce the rate of dissociation of $HNO_3$ to HONO* and also the dissociative excitation of HONO*, thus reducing sensitivity. In addition, the quenching of OH fluorescence by large concentrations of $HNO_3$ can also act in the same direction, both effects resulting in a non- linear response of TPEFS as a function of [$HNO_3$] as exemplified in Fig. S1, which displays the variation of the TPEFS signal with [$HNO_3$] at two different total pressures. Even though we were able to parametrize the TPEFS signal over a wide range of [$HNO_3$] (up to $10^{16}$ molecule $cm^{-3}$) and pressures (25 to 150 Torr $N_2$) we performed most of these experiments at constant [$HNO_3$] and densities to simplify the analysis.

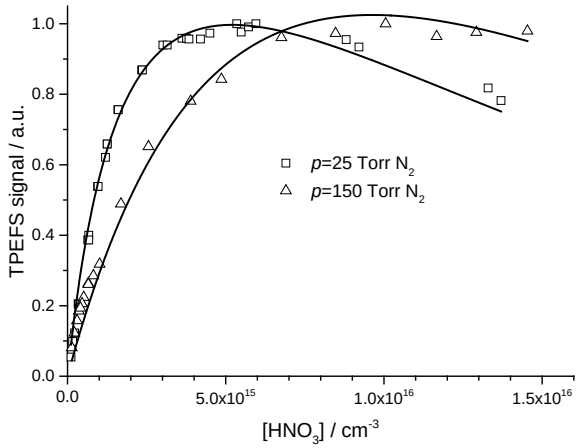


**Figure S1**. Dependence of the TPEFS signal on [$HNO_3$] at $p$=25 and 150 Torr $N_2$ at room temperature. Solid lines corresponds to a global fit using eq. (S1) where $l$ = 5 cm (fixed), $k_{N2}$=1.3 $10^{-11}$ $cm^3$ $molecule^{-1}$ $s^{-1}$ (fixed) and $k_{HNO3}$=5.4 $10^{-9}$ $cm^3$ $molecule^{-1}$ $s^{-1}$ (varied).

The TPEFS signal is given by the following expression,

$$S_{TPEFS} = C \cdot N \cdot \frac{I}{I_0} \cdot [\mathrm{HNO_3}] \cdot \phi \qquad (1)$$

Where $C$ is a calibration factor (dependent on PMT characteristics, fluorescence collection efficiency etc.), $N$ is the photon density in photon/$cm^2$, $I$ / $I_0$ is the fraction of the 193 nm photons that reach the centre of the reaction cell:

$$\frac{I}{I_0} = e^{-(\sigma_{193nm}[\mathrm{HNO_3}]l)} \qquad (2)$$

where $\sigma_{193\,nm}$ is the cross-section of $HNO_3$ at 193 nm ($1.15 \times 10^{-17}$ $cm^2$ $molecule^{-1}$)[8], $l$ is the absorption length in cm and $\phi$ is the fluorescence yield:

$$\phi = \frac{kf}{kf + k_{N2}[N_2] + k_{HNO3}[HNO_3]} \quad (3)$$

where $k_f$ is the OH fluorescence rate constant in $s^{-1}$ ($1.5\ 10^6$ $s^{-1}$) (German, 1975), $k_{N2}$ and $k_{HNO3}$ are the quenching rate coefficient (in $cm^3$ $molecule^{-1}$ $s^{-1}$) of $N_2$ and $HNO_3$ respectively.

Of the parameters given above, the absorption length and the quenching rate coefficients for $N_2$ and $HNO_3$ needed to be determined. We measured the absorption length by recording the 193 nm light attenuation as a function of $[HNO_3]$ (see Figure S3) using a Joule meter placed at the rear of the reactor. The Joule meter signal as a function of $[HNO_3]$ was fitted to the Beer-Lambert law (eq. 2) and an absorption length of ≈ 10 cm was obtained. The fluorescence is detected in the middle of the reactor and so the absorption length $l$ in eq. (1) is ≈ 5 cm.

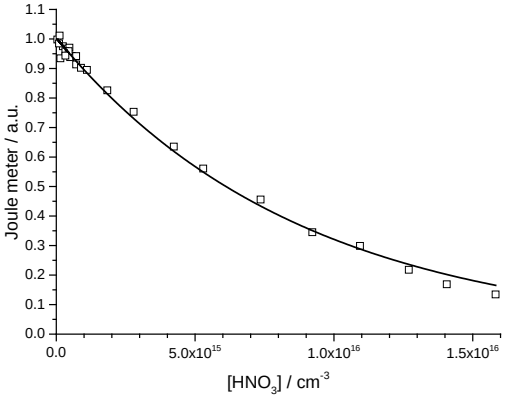


**Figure S2**. Extinction of 193 nm light by $[HNO_3]$. The effective path-length for absorption was calculated using the literature cross-section of $HNO_3$ at 193 nm.

The rate constant for OH(A) quenching by $N_2$ ($k_{N2}$), determined by varying the $N_2$ pressure at constant $HNO_3$ concentration at room temperature, was found to be $1.3 \times 10^{-11}$ $cm^3$ $molecule^{-1}$ $s^{-1}$, which is in excellent agreement with Kenner et al. (1986).

The rate constant for OH(A) quenching by $HNO_3$ ($k_{HNO3}$) is reported to be $5.9 \times 10^{-10}$ $cm^3$ $molecule^{-1}$ $s^{-1}$ (Kenner et al., 1986). Using these parameters does however not reproduce the strong $HNO_3$ dependence at $[HNO_3] > 10^{15}$ $cm^{-3}$ and a value of $k_{HNO3}$ of $5.4 \times 10^{-9}$ $cm^3$ $molecule^{-1}$ $s^{-1}$ better reproduces our observations. The difference between the value we require to match our observations and the literature rate constant for $k_{HNO3}$ indicates that the expression used here to describe the TPEFS signal as a function of $[HNO_3]$ is an approximation that does not include for example the effect of $N_2$ and $HNO_3$ on the energy transfer from highly excited vibrational states of the first electronic state down to OH(A) v'=0. Also, we simplified the expression to a one-absorption phenomenon where OH(A) is actually the result of a 2-photon sequential

absorption process. The parametrized expression is however sufficient to reproduce our experimentally observed dependence of the TPEFS signal on [$HNO_3$] (see Figure S1).

We also explored the temperature dependence of the $N_2$ quenching rate of OH(A) in an experiment with constant [$HNO_3$] and constant [$N_2$]. The first order decay constant for the OH fluorescence was derived by fitting a single exponential decay to the raw signal recorded by a 100 MHz oscilloscope.

We found no significant change in the OH fluorescence decay rate as we lowered the temperature (see Figure S3), which contrasts the weak dependence observed for OH quenching from (A, v´=0) due to collisions with $N_2$ (dashed line in Figure S4) (Copeland and Crosley, 1986). The difference is likely related to the fact that nascent OH generated in the two-photon excitation of $HNO_3$ is very hot, with an approximate vibrational temperature of 3200 K and rotational temperature of 700 K. As the required rate constant for quenching by $HNO_3$ exceeds $10^{-9}$ $cm^3$ $molecule^{-1}$ $s^{-1}$, we assume that this parameter is, to a good approximation, independent of temperature.

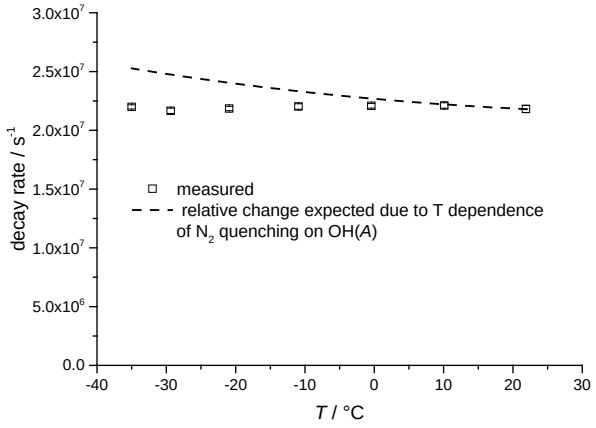


**Figure S3**. OH fluorescence decay rate as a function of temperature. Conditions: pressure = 50 Torr $N_2$ and [$HNO_3$] = 2.7 $10^{15}$ molecule $cm^{-3}$

**References**

Kenner, R. D., Rohrer, F., Papenbrock, T., and Stuhl, F.: Excitation mechanism for OH(A) in the ArF excimer laser photolysis of nitric acid. J. Phys. Chem., 90, 1294-1299, doi:10.1021/j100398a018, 1986.

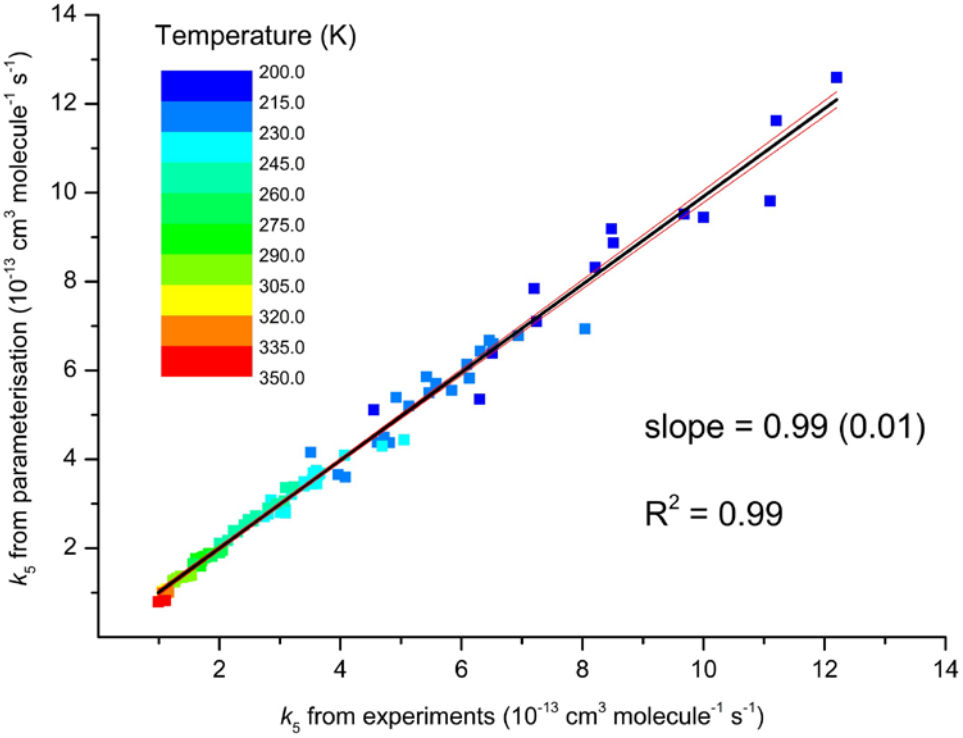


**Figure S4**. Experimentally determined values of $k_5$ at various temperatures and pressures compared to the values obtained using the expression (iii), $k_5 = k + k_\Delta / (1 + k_\Delta / k_c[M])$ with $k = 1.32 \times 10^{-14}$ exp (527/$T$) cm$^3$ molecule$^{-1}$ s$^{-1}$, $k_\Delta = 9.73 \times 10^{-17}$ exp (1910/$T$) cm$^3$ molecule$^{-1}$ s$^{-1}$ and $k_c = 7.39 \times 10^{-32}$ exp (453/$T$) cm$^6$ molecule$^{-2}$ s$^{-1}$. The black line is the linear fit to the data (slope = 0.99 ± 0.01), R2 = 0.99 and the red lines are the 95 % confidence limits.

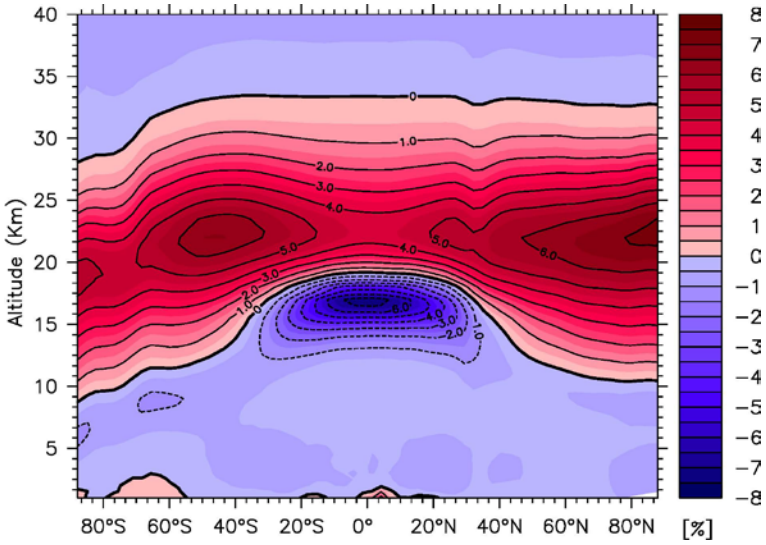


**Figure S5**. Modelled changes (%) in the $NO_x$ / $HNO_3$ ratio resulting from the new parameterisation of $k_5$.